ISSN 1674-1056
http://cpb.iphy.ac.cn
http://iopscience.iop.org/cpb
中国物理 B
Chinese Physics
中国物理 Chinese Physics B

Finite-dimensional pair coherent state engendered via the nonlinear Bose operator realization and its Wigner phase-space distributions

Jianming Liu(刘建明)[1], Xiangguo Meng(孟祥国)[2]

Citation: Chin. Phys. B . 2019, 28(12): 124206 . **doi:** 10.1088/1674-1056/ab4f5f
Journal homepage: http://cpb.iphy.ac.cn; http://iopscience.iop.org/cpb

What follows is a list of articles you may be interested in

Double-passage mechanical cooling in a coupled optomechanical system

Qing-Xia Mu(穆青霞)[1], Chao Lang(郎潮)[1], Wen-Zhao Zhang(张闻钊)[2]

Chin. Phys. B . 2019, 28(11): 114206 . **doi:** 10.1088/1674-1056/ab48f1

Analytic solutions for generalized *PT*-symmetric Rabi models

Yuanhao Dong(董元浩)[1], Wen-Jing Zhang(张文静)[2], Jing Liu(刘静)[1], Xiao-Tao Xie(谢小涛)[1]

Chin. Phys. B . 2019, 28(11): 114202 . **doi:** 10.1088/1674-1056/ab457b

Generation of entangled TEM_{01} modes withperiodically poled $KTiOPO_4$ crystal

Rong-Guo Yang(杨荣国), Jing-jing Wang(王晶静), Jing Zhang(张静), Heng-Xin Sun(孙恒信)

Chin. Phys. B . 2016, 25(7): 074208 . **doi:** 10.1088/1674-1056/25/7/074208

Photon-number distribution of two-mode squeezed thermal states by entangled state representation

Hu Li-Yun, Wang Shuai, Zhang Zhi-Ming

Chin. Phys. B . 2012, 21(6): 064207 . **doi:** 10.1088/1674-1056/21/6/064207

A simple scheme to generate *χ*-type four-charge entangled states in circuit QED

Gao Gui-Long,Song Fu-Quan,Huang Shou-Sheng,Wang Hui,Yuan Xian-Zhang,Wang Ming-Feng,Jiang Nian-Quan

Chin. Phys. B . 2012, 21(4): 044209 . **doi:** 10.1088/1674-1056/21/4/044209

Finite-dimensional pair coherent state engendered via the nonlinear Bose operator realization and its Wigner phase-space distributions

Jianming Liu(刘建明)[1,†] and Xiangguo Meng(孟祥国)[2,‡]

[1] Department of Computer, Weifang Medical University, Weifang 261000, China
[2] Shandong Provincial Key Laboratory of Optical Communication Science and Technology, School of Physical Science and Information Engineering, Liaocheng University, Liaocheng 252059, China

(Received 22 September 2019; revised manuscript received 11 October 2019; published online 15 November 2019)

We theoretically analyze the photon number distribution, entanglement entropy, and Wigner phase-space distribution, considering the finite-dimensional pair coherent state (FDPCS) generated in the nonlinear Bose operator realization. Our results show that the photon number distribution is governed by the two-mode photon number sum q of the FDPCS, the entanglement of the FDPCS always increases quickly at first and then decreases slowly for any q, and the nonclassicality of the FDPCS for odd q is more stronger than that for even q.

Keywords: finite-dimensional pair coherent state, entangled state

PACS: 42.50.−p, 05.30.−d, 03.65.−w **DOI:** 10.1088/1674-1056/ab4f5f

1. Introduction

Non-Gaussian entangled states (NGESs) as a new physical carrier can be very useful in both theoretical and experimental aspects of quantum information mainly because such states can overcome the shortage of the local Gaussian unitary operations and their induced Gaussian states.[1–3] Especially, the NGESs effectively improve some certain quantum information protocols including quantum teleportation,[4] quantum key distribution,[5] and quantum metrology.[6–8]

Among all the NGESs, pair coherent states (PCSs) have some prominent nonclassical properties including squeezing and sub-Poissionian distribution,[9] entanglement quantified via quantum Fisher information or Neumann entropy, and nonlocality.[10] Hence, it is a valuable quantum information resource which can be widely used to realize or improve quantum interferometric lithography,[11] quantum teleportation,[12] Heisenberg-limited interferometry,[13] and measurement-device-independent quantum key distribution.[14,15] Experimentally, the PCSs can be generated in an idealistic scenario via weak cross-Kerr media, the competition of four-wave mixing and amplified spontaneous emission,[16] the motion of an ion in a two-dimensional trap,[17] the nondegenerate parametric oscillator,[18] or state-projective scheme in traveling-wave optical fields.[19] In addition, the PCSs can be used to prepare some useful quantum states, such as Schröinger cat states,[20] superpositions of PCSs,[21] generalized PCSs[22,23] and quantum mixture coming from phase randomization of a PCS.[10]

As an induced NGES of the PCS, in this paper we introduce the finite-dimensional pair coherent state (FDPCS) in the nonlinear Bose operator realization and investigate its entanglement and nonclassicality via the photon number distribution (PND), entangled entropy, and Wigner function (WF), and detailedly discuss how the controlled parameters q (i.e., two-mode photon number sum) and τ influence them. The work is arranged as follows. In Section 2 the FDPCS is theoretically generated via the nonlinear Bose operator realization. In Sections 3 and 4 the PND of the FDPCS is numerically examined in the two-mode Fock space and the entanglement degree of the FDPCS is quantified via its Neumann entropy. Section 5 is devoted to using two conjugated entangled state representations to analytically derive the WF for the FDPCS and its marginal distribution functions, and investigate the nonclassicality of the FDPCS in terms of the partial negativity of the WF. Some main results are summarized in Section 6.

2. Finite-dimensional pair coherent state

Notice that the nonlinear Bose operator realization of $SU(2)$ generators gives

$$\begin{aligned} Y_+ &= \frac{1}{n_a+1}ab^\dagger, \\ Y_- &= a^\dagger b(n_a+1), \\ Y_0 &= \frac{1}{2}(b^\dagger b - a^\dagger a), \end{aligned} \tag{1}$$

where the operators a and b are the bosonic annihilation operators of two-mode optical fields, which can annihilate the vacuum state $|0,0\rangle$, $n_a = a^\dagger a$ is the particle-number operator of a-mode, and the generators $Y_\pm$ and Y_0 yield the following $SU(2)$ Lie algebra:

$$[Y_+, Y_-] = 2Y_0, \quad [Y_0, Y_\pm] = \pm Y_\pm. \tag{2}$$

†Corresponding author. E-mail: sdwfljm@126.com
‡Corresponding author. E-mail: mengxiangguo1978@sina.com

© 2019 Chinese Physical Society and IOP Publishing Ltd

Thus we can define a unitary evolution operator $\mathfrak{U}(\xi) = \exp(\xi Y_+ - \xi^* Y_-)$, whose standard factorization is

$$\mathfrak{U}(\xi) = \exp(\tau Y_+)\exp\left[Y_0 \ln(1+|\tau|^2)\right]\exp(-\tau^* Y_-), \quad (3)$$

where $\tau = \mathrm{e}^{-\mathrm{i}\phi}\mathrm{tg}\frac{\theta}{2}$ and $\xi = \frac{\theta}{2}\mathrm{e}^{-\mathrm{i}\phi}$. Hence, operating the exponential operator $\mathfrak{U}(\xi)$ in Eq. (3) on the two-mode number states $|q,0\rangle$ leads to the FDPCS, that is,

$$\begin{aligned} |\xi,q\rangle &= \mathfrak{U}(\xi)|q,0\rangle \\ &= \mathscr{N}_{\tau,q}^{-1/2}\sum_{n=0}^{q}\tau^n\sqrt{\frac{(q-n)!}{q!n!}}|q-n,n\rangle, \end{aligned} \quad (4)$$

which is the same form as Ref. [24]. Here $\mathscr{N}_{\tau,q}$ is the normalization factor, i.e., $\mathscr{N}_{\tau,q} = \sum_{n=0}^{q}|\tau|^{2n}\frac{(q-n)!}{q!n!}$. Indeed, it yields the following eigenvector equations:

$$\begin{aligned} \left(a^\dagger b + \frac{\xi^{q+1}(ab^\dagger)^q}{(q!)^2}\right)|\xi,q\rangle &= \xi|\xi,q\rangle, \\ (a^\dagger a + b^\dagger b)|\xi,q\rangle &= q|\xi,q\rangle. \end{aligned} \quad (5)$$

In theoretical generating scheme, the FDPCS can be produced in the vibrational motion process of a trapped ion in a two-dimensional harmonic potential.[24]

3. Photon number distribution

As a vital quantum feature of the state $|\xi,q\rangle$, its PND ($|\langle n_a,n_b|\xi,q\rangle|^2$) means the probabilities of finding (n_a,n_b) photons in this optical field.[25,26] Hence, we now calculate the PND of the state $|\xi,q\rangle$ as

$$P(n_a,n_b) = \mathscr{N}_{\tau,q}^{-1}\frac{(q-n_b)!}{q!n_b!}|\tau|^{2n_b}\delta_{q-n_b,n_a}, \quad (6)$$

which means that the PND is constrained by the condition $n_a = q - n_b$. In other words, the probabilities of finding only several (n_a,n_b) numbers of photons in the state $|\xi,q\rangle$ cannot be zero because of the restrictive condition $n_a + n_b = q$, however the PND always becomes zero when $n_a \neq q - n_b$. This seems understandable because the two-mode photon number sum of the state $|\xi,q\rangle$ is just equal to q.

In Fig. 1, we present the PND $P(n_a,n_b)$ of the state $|\xi,q\rangle$ in the Fock space (n_a,n_b) for different parameters q and τ. From Fig. 1, it is clearly seen that the PND only emerges in several (n_a,n_b) numbers of photons and is equal to zero for other photon numbers since it is restricted from the condition $n_a + n_b = q$, as the above analytical result in Eq. (6). For a smaller value of q, the maximum probability of finding photons appears where n_b takes a maximum value (or n_a takes a minimum value). As the parameter q increases, more photons appear in number states with smaller n_b, thus the maximum probability of finding (n_a,n_b) photons gradually decreases and moves only along the diagonal direction toward the larger n_a numbers of photons [see Figs. 1(a)–1(c)]. However, the changes of the PND with the increase of the parameter τ are just contrary [see Figs. 1(d)–1(f)]. Overall, the values of the parameters q and τ directly affect the positions and values of the peaks of the PND.

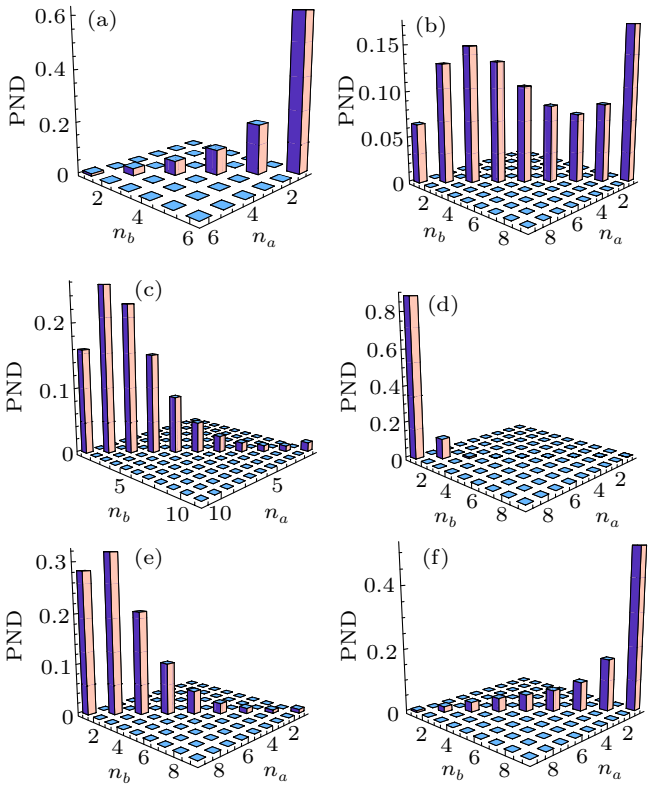


Fig. 1. Photon number distribution $P(n_a,n_b)$ of the FDPCS in the two-mode Fock space (n_a,n_b) for some different values of (q,τ), where $(5,4)$, $(8,4)$, $(10,4)$, $(8,1)$, $(8,3)$, and $(8,5)$, respectively, refer to (a), (b), (c), (d), (e), and (f).

4. Entanglement

In the present section, we quantify the degree of quantum entanglement of the FDPCS via computing its Neumann entropy. For a pure bipartite entangled state $|\varphi\rangle_{ab}$ with the Schmidt decomposition, i.e., $|\varphi\rangle_{ab} = \sum_{n=1} d_n|\alpha_n\rangle_a|\beta_n\rangle_b$, where the states $|\alpha_n\rangle_a, |\beta_n\rangle_b$ are mutually orthonormal and d_n is positive and real. Hence, its entanglement degree can be characterized via the partial Neumann entropy of the reduced density operator, i.e., $E(|\varphi\rangle_{ab}) = -\mathrm{tr}(\rho_a\ln\rho_a) = -\sum_{n=1} d_n^2\log_2 d_n^2$, where $\rho_a = \mathrm{tr}_b(|\varphi\rangle_{ab}\langle\varphi|)$.[27–30] Using the Schmidt expansion of the state $|\xi,q\rangle$ in Eq. (4), and thus its entanglement entropy can be easily calculated by

$$E = -\sum_{n=0}^{q}\frac{(q-n)!|\tau|^{2n}}{\mathscr{N}_{\tau,q}q!n!}\log_2\frac{(q-n)!|\tau|^{2n}}{\mathscr{N}_{\tau,q}q!n!}. \quad (7)$$

In Fig. 2, we present the entanglement entropy of the FDPCS as a function of the parameter τ for different values of q. Obviously, for any q, the entanglement of the FDPCS always increases very quickly at first stage of the parameter τ

and then decreases slowly for the remaining stages as τ is increased, and is always close to zero when τ is large enough. However, for a large value of q, the entanglement tends to zero more slowly. When a threshold of the parameter τ is reached, the maximum value of the entanglement is shown. Also, as q increases, the threshold of τ and the maximum value of the entanglement gradually increases.

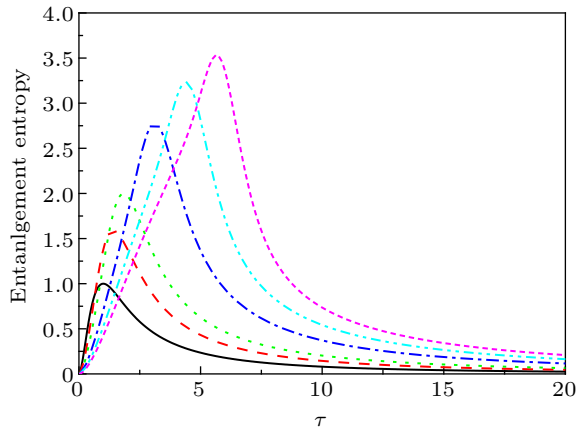


Fig. 2. Entanglement entropy of the FDPCS as a function of the parameter τ for $q=1$ (black solid line), $q=2$ (red dashed line), $q=4$ (green dotted line), $q=6$ (blue dash-dotted line), $q=9$ (cyan dash-dot-dotted line), $q=12$ (magenta short-dashed line).

5. Wigner phase-space distributions

In quantum statistical theory, the WF of quantum state in phase space contains some crucial information of this state, especially its quantum interference character and partial negativity can frequently be used to accurately describe the nonclassicality of the state. Hence, in this section we analytically and numerically study the Wigner phase-space distributions for the FDPCS.

5.1. Two conjugated entangled states

To derive the WF for the state $|\xi,q\rangle$, we next review two conjugated two-mode entangled states $|\rho\rangle$ and $|\vartheta\rangle$ and their main properties. In Refs. [31] and [32] the authors pointed out that the entangled state $|\rho\rangle$ simultaneously obeys the eigenequations

$$\left(a+b^{\dagger}\right)|\rho\rangle=\rho\,|\rho\rangle\,,\ \left(b+a^{\dagger}\right)|\rho\rangle=\rho^{*}\,|\rho\rangle \tag{8}$$

because of the communative relation $[a+b^{\dagger},b+a^{\dagger}]=0$, or the states $|\rho\rangle$ are the common eigenstates of the relative coordinate operator (Q_a-Q_b) and the total momentum operator (P_a+P_b), i.e.,

$$\begin{aligned}(Q_a-Q_b)\,|\rho\rangle &= \sqrt{2}\rho_1\,|\rho\rangle\,,\\ (P_a+P_b)\,|\rho\rangle &= \sqrt{2}\rho_2\,|\rho\rangle\,,\end{aligned} \tag{9}$$

where $Q_i=(i+i^{\dagger})/\sqrt{2}$, $P_i=(i-i^{\dagger})/(\mathrm{i}\sqrt{2})$, $(i=a,b)$, thus $|\rho\rangle$ represents an entangled state defined as in two-mode Fock space[32–34]

$$|\rho\rangle=\mathrm{e}^{-\frac{1}{2}|\rho|^2+\rho a^{\dagger}-\rho^{*}b^{\dagger}+a^{\dagger}b^{\dagger}}\,|0,0\rangle\,, \tag{10}$$

where ρ is a complex parameter, $\rho=\rho_1+\mathrm{i}\rho_2$. In term of Eq. (10), and using the normal ordering of two-mode vacuum projection operator[35,36] and the integration technique within an ordered operator product (IWOP),[37,38] we can prove the completeness relation of the state $|\rho\rangle$, i.e., $\int\frac{\mathrm{d}^2\rho}{\pi}\,|\rho\rangle\langle\rho|=1$, and its orthonormalized property, i.e., $\langle\rho|\,\rho'\rangle=\pi\delta^{(2)}(\rho-\rho')$. Further, using the generating function of two-variable Hermite polynomials $H_{m,n}(\varepsilon,\varepsilon^{*})$, we have

$$\sum_{m,n=0}^{\infty}\frac{t^m t'^n}{m!n!}H_{m,n}(\varepsilon,\varepsilon^{*})=\exp\left(-tt'+t\varepsilon+t'\varepsilon^{*}\right). \tag{11}$$

We can obtain the expansion of the entangled state $|\rho\rangle$ under the basis of two-mode number state $|m,n\rangle$, that is,

$$|\rho\rangle=\mathrm{e}^{-|\rho|^2/2}\sum_{m,n=0}^{\infty}\frac{(-1)^n H_{m,n}(\rho,\rho^{*})}{\sqrt{m!n!}}\,|m,n\rangle\,. \tag{12}$$

Similarly, another two-mode entangled state $|\vartheta\rangle$ conjugated to $|\rho\rangle$ is obtained as

$$|\vartheta\rangle=\mathrm{e}^{-\frac{1}{2}|\vartheta|^2+\vartheta a^{\dagger}+\vartheta^{*}b^{\dagger}-a^{\dagger}b^{\dagger}}\,|0,0\rangle\,, \tag{13}$$

which indeed represents the common eigenstates of the mass-center coordinate operator (Q_a+Q_b) and the relative momentum operator (P_a-P_b), i.e.,

$$\begin{aligned}(Q_a+Q_b)\,|\vartheta\rangle &= \sqrt{2}\vartheta_1\,|\vartheta\rangle\,,\\ (P_a-P_b)\,|\vartheta\rangle &= \sqrt{2}\vartheta_2\,|\vartheta\rangle\,.\end{aligned} \tag{14}$$

Its expansion in two-mode Fock space is expressed as

$$|\vartheta\rangle=\mathrm{e}^{-|\vartheta|^2/2}\sum_{m,n=0}^{\infty}\frac{H_{m,n}(\vartheta,\vartheta^{*})}{\sqrt{m!n!}}\,|m,n\rangle\,, \tag{15}$$

and there exists the relation between $|\vartheta\rangle$ and $|\rho\rangle$, i.e., $|\vartheta\rangle=(-1)^{a^{\dagger}a}\,|\rho=-\vartheta\rangle$.

5.2. Partial negativity of Wigner function

In the two-mode entangled state $|\rho\rangle$ representation, the two-mode Wigner operator is neatly expressed as[39–41]

$$\Delta(\varsigma,\sigma)=\int\frac{\mathrm{d}^2\rho}{\pi^3}\,|\varsigma-\rho\rangle\langle\varsigma+\rho|\exp\left(\rho\sigma^{*}-\rho^{*}\sigma\right), \tag{16}$$

where ς and σ are complex parameters. Indeed, using Eqs. (10), (16) and the IWOP method, we can find the identity $\Delta(\varsigma,\sigma)=\Delta(\alpha)\otimes\Delta(\beta)$ via letting $\sigma=\alpha+\mathrm{i}\beta^{*}$, $\varsigma=\alpha-\mathrm{i}\beta^{*}$ in Eq. (16), where $\Delta(\alpha)$ and $\Delta(\beta)$ are two independent single-mode Wigner operators.[42,43] Hence, the WF for the FDPCS reads

$$W(\varsigma,\sigma)=\mathrm{Tr}\left[\Delta(\varsigma,\sigma)\,|\xi,q\rangle\langle\xi,q|\right]. \tag{17}$$

Combining Eqs. (4) and (12), we calculate the scalar product $\langle\rho\,|\xi,q\rangle$ as

$$\langle\rho\,|\xi,q\rangle=\mathscr{N}_{\tau,q}^{-1/2}\mathrm{e}^{-|\rho|^2/2}\sum_{n=0}^{q}\frac{(-\tau)^n H_{q-n,n}(\rho^{*},\rho)}{n!\sqrt{q!}}, \tag{18}$$

thus the function $W(\varsigma,\sigma)$ is obtained as

$$W(\varsigma,\sigma) = \frac{\mathrm{e}^{-|\varsigma|^2}}{\mathscr{N}_{\tau,q}} \sum_{m,n=0}^{q} \frac{(-1)^{m+n}\tau^{*m}\tau^{n}}{m!n!q!} \int \frac{\mathrm{d}^2\rho}{\pi^3} \times H_{q-m,m}(\varsigma-\rho,\varsigma^*-\rho^*) H_{n,q-n}(\varsigma+\rho,\varsigma^*+\rho^*) \times \exp\left(-|\rho|^2+\rho\sigma^*-\rho^*\sigma\right). \quad (19)$$

Further, using the power-series expansion of $H_{m,n}(\varepsilon,\varepsilon^*)$,[44,45]

$$H_{m,n}(\varepsilon,\varepsilon^*) = \sum_{l=0}^{\min(m,n)} \frac{(-)^l n!m!\varepsilon^{m-l}\varepsilon^{*n-l}}{l!(m-l)!(n-l)!} = \frac{\partial^{m+n}}{\partial t^m \partial t'^n} \exp\left(-tt'+t\varepsilon+t'\varepsilon^*\right)\Big|_{t=t'=0}, \quad (20)$$

and the mathematics integration formula[42,46,48]

$$\int \frac{\mathrm{d}^2 z}{\pi} \mathrm{e}^{\zeta|z|^2+\xi z+\eta z^*} = -\frac{1}{\zeta}\exp\left(-\frac{\xi\eta}{\zeta}\right), \quad (21)$$

which holds for the constrained condition $\mathrm{Re}\zeta < 0$, thus we have

$$W(\varsigma,\sigma) = \frac{\mathrm{e}^{-|\sigma|^2-|\varsigma|^2}}{\pi^2\mathscr{N}_{\tau,q}} \sum_{m,n=0}^{q} \frac{(-1)^{m+n}\tau^{*m}\tau^{n}}{m!n!q!} \times H_{q-m,q-n}(\upsilon,\upsilon^*) H_{n,m}(\varkappa,\varkappa^*), \quad (22)$$

where $\varkappa = \varsigma - \sigma$ and $\upsilon = \varsigma + \sigma$. It shows that the function $W(\varsigma,\sigma)$ is related to two-variable Hermite polynomials with the maximum order q. In terms of the standard definition of $H_{m,n}(\cdot,\cdot)$ and the exponential term $(-1)^{m+n}$, we decide that the function $W(\varsigma,\sigma)$ can show some negative regions in the whole phase space for some certain values of the parameters q and τ, as an evidence of the nonclassicality of the FDPCS.

In Fig. 3, we present the WF $W(\varsigma,\sigma)$ for the FDPCS as a function of $\mathrm{Re}\varsigma$ (taking $\mathrm{Re}\sigma = 0$) for different values of q and τ. Obviously, Figure 3(a) shows that the WF always has a upward main peak for even q but a downward main peak for odd q at the position of $\mathrm{Re}\varsigma = 0$, and for any even (or odd) q, the main peak value is unchanged, whereas the numbers and positions of the secondary peaks are completely different. However, the total number of the downward peaks is always equal to two-mode photon number sum q of the FDPCS. Intuitively, the partial negative volume of the WF for odd q is always larger than that for even q as the presence of a downward main peak for odd q, which shows that the nonclassicality of the FDPCS for odd q is stronger than that for even q. However, the nonclassicality of the FDPCS cannot monotonously change with the odd (even) q.

From Fig. 3(b), we clearly see that, for a fixed value of even q (e.g., $q = 4$), the upward main peak remains unchanged as τ increases, but the numbers and the peak values of the secondary peaks gradually decreases, even the downward secondary peaks (the partial negative volume) are completely gone and the WF becomes Gaussian when τ reaches a certain threshold value. Continuing to increase the value of τ, the downward secondary peaks representing the negative region will appear once again. This result means that the nonclassicality of the FDPCS weakens first and then enhances with the increase of τ. Especially, when the parameter τ is large or small enough, the WF has almost similar distributions, that is, the FDPCS has similar nonclassicality for the two cases. For odd q case, a similar result occurs for the FDPCS, so we ignore it here.

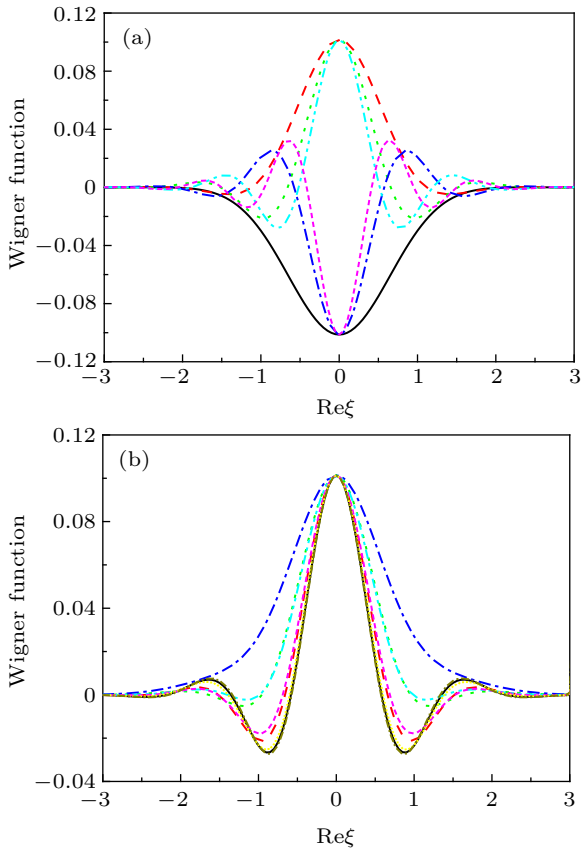


Fig. 3. Wigner function for the FDPCS of $\mathrm{Re}\varsigma$ (letting $\mathrm{Re}\sigma = 0$) for two different cases: (a) $\tau = 0.5$, and $q = 1$ (black solid line), $q = 2$ (red dashed line), $q = 4$ (green dotted line), $q = 5$ (blue dash-dotted line), $q = 6$ (cyan dash-dot-dotted line), $q = 9$ (magenta short-dashed line); (b) $q = 4$, and $\tau = 0.1$ (black solid line), $\tau = 0.5$ (red dashed line), $\tau = 1.2$ (green dotted line), $\tau = 2$ (blue dash-dotted line), $\tau = 4$ (cyan dash-dot-dotted line), $\tau = 7$ (magenta short-dashed line), $\tau = 20$ (yellow short-dotted line), $\tau = 100$ (dark-yellow short-dash-dotted line).

5.3. Marginal distribution functions

In this subsection, we want to calculate two marginal distribution functions for the function $W(\varsigma,\sigma)$ in the ς–σ phase space. Surprisingly, performing two integrations of the Wigner operator $\Delta(\varsigma,\sigma)$ over the variables σ and ς in the whole phase space, we find that the relationship between the operator $\Delta(\varsigma,\sigma)$ and two conjugate entangled states $|\rho\rangle$ and $|\vartheta\rangle$ yields[49]

$$\int \mathrm{d}^2\sigma\Delta(\varsigma,\sigma) = \frac{1}{\pi}|\rho\rangle\langle\rho|_{\rho=\varsigma},$$

$$\int \mathrm{d}^2\varsigma \Delta(\varsigma,\sigma) = \frac{1}{\pi}|\vartheta\rangle\langle\vartheta|_{\vartheta=\sigma}. \tag{23}$$

Thus, using Eqs. (4), (12) and (17), we can arrive at a marginal distribution function of $W(\varsigma,\sigma)$ in the ς variable, i.e.,

$$\begin{aligned} P(\varsigma) &= \int \mathrm{d}^2\sigma W(\varsigma,\sigma) = \frac{1}{\pi}|\langle\rho|\xi,q\rangle|^2_{\rho=\varsigma} \\ &= \frac{\mathrm{e}^{-|\varsigma|^2}}{\pi\mathscr{N}_{\tau,q}q!}\left|\sum_{n=0}^{q}\frac{(-\tau)^n H_{q-n,n}(\varsigma^*,\varsigma)}{n!}\right|^2. \end{aligned} \tag{24}$$

Similarly, using Eqs. (4), (17) and the expansion of the entangled state $|\vartheta\rangle$ in Eq. (15), we obtain another marginal distribution function of $W(\varsigma,\sigma)$ in the σ variable, that is,

$$P(\sigma) = \frac{\mathrm{e}^{-|\sigma|^2}}{\pi\mathscr{N}_{\tau,q}q!}\left|\sum_{n=0}^{q}\frac{\tau^n H_{q-n,n}(\sigma^*,\sigma)}{n!}\right|^2. \tag{25}$$

Obviously, equation (24) [or (25)] represents the probabilities for finding the two particles with the relative coordinate $\sqrt{2}\varsigma_1$ and the total momentum $\sqrt{2}\varsigma_2$ [or the mass-center coordinate $\sqrt{2}\vartheta_1$ and the relative momentum $\sqrt{2}\vartheta_2$] in the FDPCS, which is just related to the module-square of two-variable Hermite polynomials. Hence, we get a conclusion, that is, for a bipartite entangled state, the physical significance of its function $W(\varsigma,\sigma)$ is that its marginal distribution functions show the probabilities of finding two entangled particles in the ς–σ phase space.

In Fig. 4, we plot the marginal distribution functions $P(\varsigma)$ and $P(\sigma)$ for different values of q and τ. Figures 4 shows that the marginal distribution $P(\varsigma)$ [or $P(\sigma)$] is symmetrical by the axis of symmetry $\mathrm{Re}\varsigma = 0$ (or $\mathrm{Re}\sigma = 0$) and cannot monotonously change with the increase of $\mathrm{Re}\varsigma$ (or $\mathrm{Re}\sigma$). For a fixed value of τ and any q, the peak values in the distribution $P(\varsigma)$ and the valley values of $P(\varsigma)$ and $P(\sigma)$ increase first and then decreases as q increases. However, the peak values of $P(\varsigma)$ always decreases. Also, the maximum marginal distribution probability moves toward the larger $|\mathrm{Re}\varsigma|$ (or $|\mathrm{Re}\sigma|$) with the increase of q.

On the other hand, for a given q and any τ, the distributions $P(\varsigma)$ (or $P(\sigma)$) are symmetrical but cannot monotonously change with $\mathrm{Re}\varsigma$ (or $\mathrm{Re}\sigma$). Specifically, in the distribution $P(\varsigma)$, the peak values decrease first and then increase as τ increases, but the change of the valley value with τ is just contrary. However, the peak values of the distribution $P(\sigma)$ increase first and then decrease as τ increases and there exist a series of small peaks near the valley, which are different from the distribution $P(\varsigma)$. Moreover, for a large τ enough, the distributions $P(\varsigma)$ and $P(\sigma)$ are similar to those for a small τ.

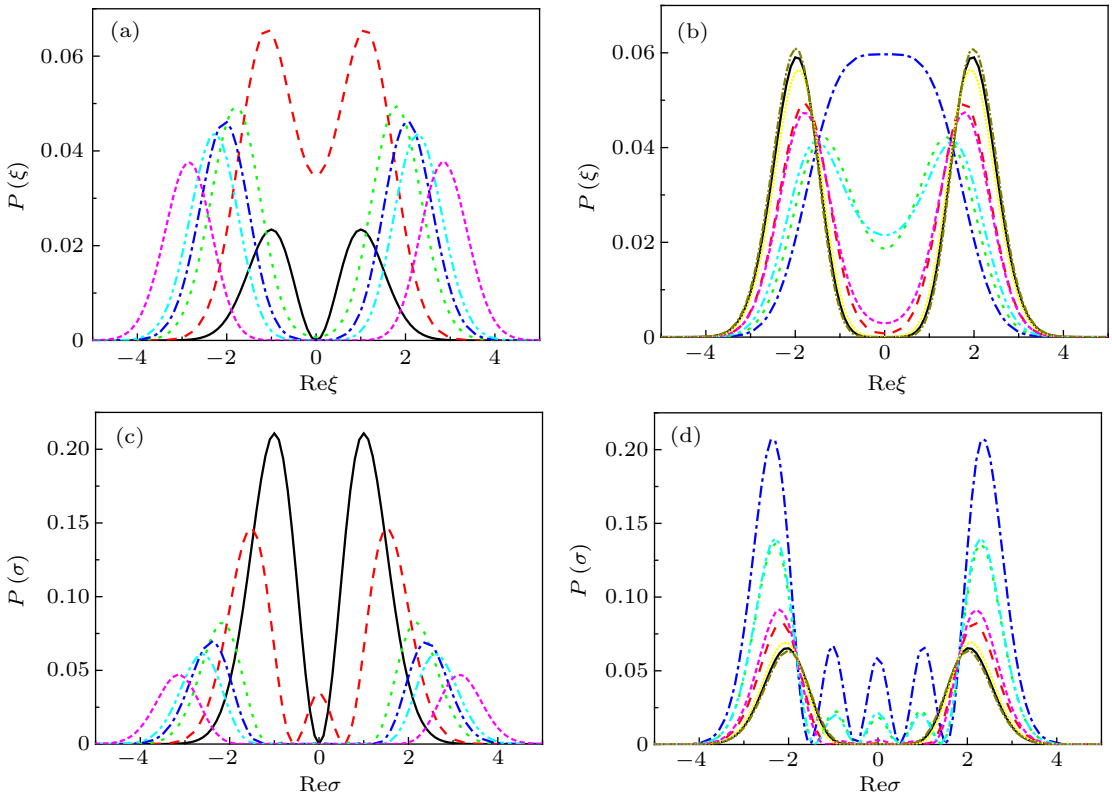


Fig. 4. Marginal distribution functions $P(\varsigma)$ and $P(\sigma)$ for the function $W(\varsigma,\sigma)$ in the ς–σ phase space for different values of q and τ, where (a) $\tau = 0.5$, and $q = 1$ (black solid line), $q = 2$ (red dashed line), $q = 4$ (green dotted line), $q = 5$ (blue dash-dotted line), $q = 6$ (cyan dash-dot-dotted line), $q = 9$ (magenta short-dashed line); (b) $q = 4$, and $\tau = 0.1$ (black solid line), $\tau = 0.5$ (red dashed line), $\tau = 1.2$ (green dotted line), $\tau = 2$ (blue dash-dotted line), $\tau = 4$ (cyan dash-dot-dotted line), $\tau = 7$ (magenta short-dashed line), $\tau = 20$ (yellow short-dotted line), $\tau = 100$ (dark-yellow short-dash-dotted line).

6. Conclusions

In summary, we have introduced the FDPCS by using the nonlinear Bose operator realization of $SU(2)$ generators and investigated its PND and entanglement entropy. It is found that the PND is restricted from the condition $n_a + n_b = q$, i.e., the two-mode photon number sum q of the FDPCS, and the parameter values of q and τ have a very different impact on the positions and values of the peak of the PND, the entanglement of the FDPCS increases in the first stage of the parameter τ and then decreases gradually for the remaining stages. Furthermore, using the entangled state $|\rho\rangle$ representation of two-mode Wigner operator, we have analytically obtained the WF for the FDPCS and its marginal distributions, and numerically discussed its nonclassical properties based on the negativity of the WF. It is shown that the FDPCS for odd q has more stronger nonclassicality than that for even q for a fixed τ, however the nonclassicality of the FDPCS decreases first and then increases with increasing τ for any q. Moreover, a fixed q and any τ, the marginal distributions $P(\varsigma)$ (or $P(\sigma)$) are symmetrical and cannot monotonously change with the parameter Reς (or Reσ).

References

[1] Eisert J, Scheel S and Plenio M B 2002 *Phys. Rev. Lett.* **89** 137903
[2] Takahashi H, Neergaard-Nielsen J S, Takeuchi M, Takeoka M, Hayasaka K, Furusawa A and Sasaki M 2010 *Nat. Photon.* **4** 178
[3] Kurochkin Y, Prasad A S and Lvovsky A I 2014 *Phys. Rev. Lett.* **112** 070402
[4] Hu L Y, Liao Z Y and Zubairy M S 2017 *Phys. Rev. A* **95** 012310
[5] Huang P, He G, Fang J and Zeng G 2013 *Phys. Rev. A* **87** 012317
[6] Carranza R and Gerry C C 2012 *J. Opt. Soc. Am. B* **29** 2581
[7] Hou L L, Sui Y X, Wang S and Xu X F 2019 *Chin. Phys. B* **28** 044203
[8] Hou L L, Xue J Z, Sui Y X and Wang S 2019 *Chin. Phys. B* **28** 094217
[9] Agarwal G S and Biswas A 2005 *J. Opt. B: Quan. Semi. Opt.* **7** 350
[10] Mancini S and Tombesi P 2003 *Quantum Inf. Comput.* **3** 106
[11] Gong Y X 2013 *Phys. Rev. A* **88** 043841
[12] Gá bris A and Agarwal G S 2007 *Int. J. Quan. Inf.* **5** 17
[13] Gerry C C and Mimih J 2010 *Phys. Rev. A* **82** 013831
[14] Zhu F, Zhang C H, Liu A P and Wang Q 2016 *Phys. Lett. A* **380** 1408
[15] Wang X, Wang Y, Chen R K, Zhou C, Li H W and Bao W S 2016 *Laser Phys.* **26** 065203
[16] Agarwal G S 1986 *Phys. Rev. Lett.* **57** 827
[17] Gou S C, Steinbach J and Knight P L 1996 *Phys. Rev. A* **54** R1014
[18] Gilchrist A and Munro W J 2000 *J. Opt. B: Quantum Semiclass. Opt.* **2** 47
[19] Gerry C C, Mimih J and Birrittella R 2011 *Phys. Rev. A* **84** 023810
[20] Gerry C C and Grobe R 1995 *Phys. Rev. A* **51** 1698
[21] Gou S C, Steinbach J and Knight P L 1996 *Phys. Rev. A* **54** 4315
[22] Chung W S and Hassanabadi H 2019 *Eur. Phys. J. Plus* **134** 394
[23] Lee C T 1990 *Phys. Rev. A* **41** 1569
[24] Obada A S F and Khalil E M 2006 *Opt. Commun.* **260** 19
[25] Meng X G, Wang J S, Liang B L and Han C X 2018 *Front. Phys.* **13** 130322
[26] Meng X G, Wang Z, Fan H Y, Wang J S and Yang Z S 2012 *J. Opt. Soc. Am. B* **29** 1844
[27] Bennett C H, Bernstein H J, Popescu S and Schumacher B 1996 *Phys. Rev. A* **53** 2046
[28] Xu X X 2015 *Phys. Rev. A* **92** 012318
[29] Li K C, Meng X G and Wang J S 2019 *Commun. Theor. Phys.* **71** 807
[30] Li K C, Meng X G and Wang J S 2019 *Int. J. Theor. Phys.* **58** 2521
[31] Fan H Y, Zaidi H R and Klauder J R 1987 *Phys. Rev. D* **35** 1831
[32] Fan H Y 2004 *Int. J. Mod. Phys. B* **18** 1387
[33] Meng X G, Liu J M, Wang J S and Fan H Y 2019 *Eur. Phys. J. D* **73** 32
[34] Fan H Y and Klauder J R 1994 *Phys. Rev. A* **49** 704
[35] Meng X G, Wang J S and Fan H Y 2011 *Opt. Commun.* **284** 2070
[36] Meng X G, Wang Z, Fan H Y and Wang J S 2012 *J. Opt. Soc. Am. B* **29** 3141
[37] Du C X, Meng X G, Zhang R and Wang J S 2017 *Chin. Phys. B* **26** 120301
[38] Wang J S, Meng X G and Fan H Y 2017 *J. Mod. Opt.* **64** 1398
[39] Meng X G, Wang Z, Wang J S and Fan H Y 2013 *J. Opt. Soc. Am. B* **30** 1614
[40] Fan H Y, Lu H L and Fan Y 2006 *Ann. Phys.* **321** 480
[41] Xu Y J and Meng X G 2019 *Laser Phys.* **29** 065002
[42] Lv H Y, Wang J S, Zhang X Y, Wu M Y, Liang B L and Meng X G 2019 *Chin. Phys. B* **28** 090302
[43] Meng X G, Goan H S, Wang J S and Zhang R 2018 *Opt. Commun.* **411** 15
[44] Wang J S, Meng X G and Fan H Y 2019 *Chin. Phys. B* **28** 100301
[45] Meng X G, Wang J S and Liang B L 2013 *Chin. Phys. B* **22** 030307
[46] Wang Z, Meng X G and Fan H Y 2013 *J. Phys. A: Math. Theor.* **46** 135305
[47] Wang Z, Meng X G and Fan H Y 2012 *J. Opt. Soc. Am. B* **29** 397
[48] Meng X G, Wang J S, Liang B L and Du C X 2018 *J. Exp. Theor. Phys.* **127** 383
[49] Meng X G, Wang J S and Liang B L 2010 *Opt. Commun.* **283** 4025